Optimal Torque Sharing-Based Direct Instantaneous Torque Control Strategy for Torque Ripple Reduction in Switched Reluctance Motors

Ameer L. Saleh
Department of Electric Power Engineering
Budapest University of Technology and Economics
H-1111 Budapest, Hungary
Department of Electrical Engineering
University of Misan, Misan, Iraq
aalkalmashi@edu.bme.hu

László Számel
Department of Electric Power Engineering
Budapest University of Technology and Economics
H-1111 Budapest, Hungary
szamel.laszlo@vik.bme.hu

2025 7th Global Power, Energy and Communication Conference (GPECOM) | 979-8-3315-1323-8/25/$31.00 ©2025 IEEE | DOI: 10.1109/GPECOM65896.2025.11061896

***Abstract*— This paper presents an enhanced Direct Instantaneous Torque Control (DITC) strategy based on an optimal Torque Sharing Function (TSF) using the Gray Wolf Optimization (GWO) algorithm to mitigate torque ripple and improve torque output, particularly in the commutation regions. The proposed approach incorporates the fast dynamic response of DITC with the smoothing capabilities of TSF to ensure effective phase torque distribution, thereby maintaining a constant instantaneous total torque. Subsequently, to further enhance torque quality and reduce the torque ripple, the TSF parameters, namely the switch-on, switch-off, and overlap angles, are optimized using the Gray Wolf Optimization (GWO) algorithm based on a multi-objective cost function that considers torque ripple minimization and improves efficiency. Simulation results validate the effectiveness of the proposed optimal TSF+DITC strategy in minimizing torque ripple and improving the overall performance of SRMs across a wide range of operating conditions. Furthermore, a comparative analysis is conducted against the optimized DITC method using a four-phase, 4 kW, 8/6 SRM prototype.**

Keywords*— *Gray wolf optimization; Direct instantaneous torque control; Switched reluctance motor; Torque sharing function.

I. INTRODUCTION

SRMs have recently been considered promising candidates that can be employed in Electric vehicles (EVs), scooters and automotive applications due to many attractive merits such as simplicity in construction with high robustness, low cost, an entire speed range capability, high starting torque, resilience to faults, and excellent energy efficiency [1]. However, SRM performance faces certain drawbacks, including torque fluctuations and magnetic nonlinearities resulting from its double salient design and switching current behavior [2]. These are the key technical limitations that restrict SRMs from being used more widely in today's technology. Recently, researchers have been focusing on overcoming these limitations by either optimizing the design parameters of the machine [3], [4], [5] or by proposing advanced torque control schemes [1], [2], [6]. Optimizing the design parameters of SRMs is effective and can lead to toque ripple minimization and reduce acoustic noise issues. But it can only do so to a limited range. On the other hand, numerous studies have demonstrated that significant reductions in torque ripple and notable improvements in machine performance can be achieved through the application of various control strategies [6], [7], [8]. These strategies are generally categorized into two main approaches: torque control and current control.

The current control methods, such as Current Chopping Control (CCC), are commonly employed in SRM drives due to their simplicity, cost-effectiveness, and operational efficiency [9]. Despite these advantages, CCC inherently generates torque ripple due to its use of square waveform for regulating phase current control without directly accounting for the resulting torque profile. This inherent drawback limits the overall performance of SRMs, restricting optimal operation to predefined switching angles associated with a fixed reference current. As a result, torque control techniques have emerged as more effective alternatives for addressing torque ripple issues [10]. The primary torque control strategies employed in SRMs to mitigate torque ripple include "Average Torque Control" (ATC), "Instantaneous Torque Control" (ITC), and "Model Predictive Torque Control" (MPTC). Each of these control approaches has benefits and drawbacks. In recent years, Instantaneous Torque Control (ITC) approaches have attracted increasing attention for their effectiveness in enhancing torque quality and significantly reducing torque ripple in SRM [11], [12]. ITC strategies are generally classified into two categories: Direct ITC (DITC) and Indirect ITC (IITC). In IITC, the torque of SRM is indirectly regulated through a cascaded control structure that converts torque references into corresponding phase currents [12]. This approach often employs Torque Sharing Functions (TSFs) to generate an optimal current profile that minimizes torque ripple. However, developing an accurate torque-to-current conversion model in practical applications remains a significant challenge. Conversely, DITC directly controls the output torque without the need for intermediate conversion, offering higher precision and faster dynamic response. DITC reacts instantaneously to torque errors by employing a torque hysteresis controller, effectively reducing torque ripples. Despite these advantages, traditional DITC still suffers from negative torque generation and residual torque ripple issues. Therefore, several schemes have been suggested to improve the DITC strategy to mitigate torque ripple further and address the current issues in this strategy. In [13], an improved DITC strategy for SRM is utilized to suppress torque ripple and increase system efficiency. The proposed approach incorporates an online optimization method for switching angles using inductance and flux linkage properties. Then, a modified commutation rule is implemented in order to minimize the toque ripple in the commutation region. In [14], an optimized DITC scheme for SRM drives is proposed using a dynamic adaptive commutation approach for torque ripple mitigation and efficiency improvement. It employs two modes for accurate torque tracking during commutation, with dynamically adjusted angles to optimize torque and minimize ripple. To address the issue of high torque ripple in PMa-SRMs, this

paper [15] proposes a novel DITC strategy incorporating zero-voltage modulation. The suggested method replaces the fixed-frequency PWM with a zero-voltage decentralized modulation scheme, optimizing the zero-voltage insertion time to minimize switching losses. Furthermore, the optimal switching angles are identified using a dung-beetle-optimized backpropagation (DBO-BP) neural network, which effectively suppresses torque ripple and boosts overall motor efficiency. An improved DITC method based on adaptive commutation angles for SRM is presented in [16]. Firstly, an Artificial Neural Network (ANN) optimized using a Modified PSO algorithm is utilized to determine the optimum switch-off angle across varying operating conditions, thereby preventing negative torque and improving average torque output and system efficiency. Then, the switch-on angle is analytically determined in each electrical cycle based on the flux derivative, ensuring full utilization of the motor's torque-producing potential. In [17], A novel DITC strategy based on PWM for SRM was suggested in order to suppress torque ripple effectively. This approach employs PWM to regulate torque deviation. Optimal switching signals are generated based on both the PWM modulation signal and the rotor's positional sector.

On the other hand, researchers recently have put forward various approaches to overcome the challenges of conventional DITC in SRM, particularly in minimizing high torque ripple and improving efficiency, which established an integration of the DITC strategy with the TSF approach to improve the performance of the DITC strategy. In [18], an enhanced DITC strategy incorporating an adaptive switch-on angle-TSF approach. The suggested approach integrates TSF into the control scheme and divides each electrical cycle into six distinct sectors, assigning appropriate candidate voltage states to each. This scheme enables effective torque ripple suppression and improves overall efficiency under varying operating conditions. In [19], this study introduced a DITC strategy augmented by an optimized Torque Sharing Function (TSF) based on commutation angles. First, an enhanced cosine-based TSF was designed to efficiently distribute the total reference torque across motor phases, ensuring stable torque synthesis during commutation. To further optimize performance, a modified Artificial Bee Colony (ABC) algorithm was implemented to identify the ideal switching angles for various operating speeds. In [20], a novel Adaptive Takagi-Sugeno-Kang (TSK) Fuzzy Sliding Mode Controller (AFSC) is suggested for an improved DITC approach for SRM. The Sliding Mode Controller (SMC) is employed to enhance system robustness by mitigating the effects of uncertainties and external disturbances while ensuring rapid dynamic response. Reference [21] proposes an enhanced fuzzy controller incorporating the Torque Sharing Function (TSF) method to improve the speed controller's dynamic performance and mitigate torque ripple in SRMs. The strategy combines fuzzy logic with standard PID control, enabling autonomous proportional gain adaptation. Specifically, when the speed error is large, fuzzy control is activated to provide a rapid response.

This paper proposed an enhanced DITC strategy based on optimal TSF. Firstly, the TSF is suggested into the traditional DITC system to minimize torque ripple in commutation overlap regions. Secondly, the control parameters of TSF are optimized using a grey wolf algorithm based on a multi-objective function to achieve accurate torque tracking while minimizing the torque ripple. The simulation results prove that the suggested method achieved the main goal of the incorporation between TSF and DITC, especially minimizing the torque ripple in the overlap region.

II. Proposed Torque Control Strategy

A. Conventional DITC Strategy

The DITC strategy is a considerably effective solution for minimizing the torque ripple and overcoming the limitations commonly encountered in indirect torque control approaches [14]. Furthermore, DITC demonstrates exceptional dynamic performance by enabling real-time error elimination. The control scheme continuously estimates instantaneous torque and compares it with the reference torque to generate the torque error signal (ΔT), which is used directly as the control input variable. This method eliminates the need for a current control loop by employing a torque hysteresis controller to generate suitable switching signals for the asymmetric half-bridge converter (AHBC), as shown in Fig. 1[16]. The generated switching signals include three modes: excitation mode, freewheeling mode, and demagnetization mode and the voltage of the k-phase winding under the soft-chopping scheme is expressed as follows:

$$U_k = \begin{cases} U_{\mathrm{dc}}, & S_1 \text{ on}, \quad S_2 \text{ on} \rightarrow \text{Excitation mode} \\ 0, & S_1 \text{ off}, \quad S_2 \text{ on} \rightarrow \text{Freewheeling mode} \\ -U_{\mathrm{ds}}, & S_1 \text{ off}, \quad S_2 \text{ off} \rightarrow \text{Demagnetization mode} \end{cases} \quad (1)$$

where S_1 and S_2 represent the drive signals for the upper and lower switches for k-phase, U_{dc} is the supplied dc voltage, and U_k is the voltage of k-phase.

However, the conventional DITC approach exhibits significant torque ripple under high-speed or heavy-load conditions, primarily due to the challenge of maintaining a balance between the instantaneous and reference torque when fixed excitation angles are employed. To address this problem, this work proposes an enhanced DITC strategy using an optimal TSF and the Gray Wolf Optimization (GWO) algorithm.

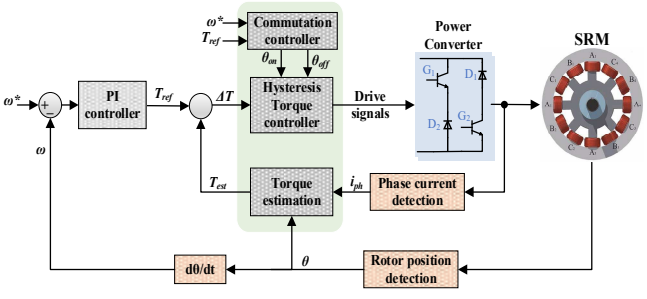

Fig. 1. Conventional DITC Strategy

B. Torque Sharing Function

The "Torque Sharing Function" (TSF) is an effective approach for mitigating torque ripple and can be integrated with other control strategies to enhance performance. The primary objective of the TSF strategy is to maintain a constant total output torque by appropriately adjusting the

torque contribution of each phase [22]. In this work, a cosine-based TSF is employed to distribute the total reference torque among the motor phases based on rotor position and phase. Fig. 2 demonstrates the waveform of the cosine TSF, and the functions are defined in equation (2).

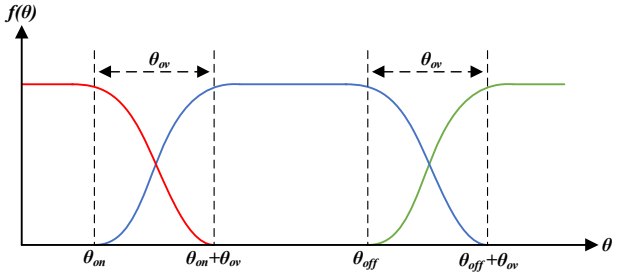

Fig. 2. Waveform of the cosine TSF.

$$T_{\mathrm{k}}^{*}(\theta)=\begin{cases}0 & (0\le\theta<\theta_{\mathrm{on}})\\ T_{\mathrm{e}}^{*}\cdot f_{\mathrm{rise}}(\theta) & (\theta_{\mathrm{on}}\le\theta<\theta_{\mathrm{on}}+\theta_{\mathrm{ov}})\\ T_{\mathrm{e}}^{*} & (\theta_{\mathrm{on}}+\theta_{\mathrm{ov}}\le\theta<\theta_{\mathrm{off}})\\ T_{\mathrm{e}}^{*}\cdot f_{\mathrm{fall}}(\theta) & (\theta_{\mathrm{off}}\le\theta<\theta_{\mathrm{off}}+\theta_{\mathrm{ov}})\\ 0 & (\theta_{\mathrm{off}}+\theta_{\mathrm{ov}}\le\theta<\theta_{\mathrm{p}})\end{cases} \quad (2)$$

Where $T_{\mathrm{k}}^{*}(\mathrm{p}=\mathrm{a},\mathrm{b},\mathrm{c},\mathrm{d})$ is the reference torque of each phase, T_{e}^{*} is the total reference torque. The relationship between $f_{\mathrm{rise}}(\theta)$ and $f_{\mathrm{fall}}(\theta)$ at the overlap region of the cosine TSF can be obtained by (3):

$$\begin{cases}f_{\mathrm{rise}}(\theta)=\frac{T^{*}}{2}-\frac{T^{*}}{2}\cos\frac{\pi}{\theta_{ov}}(\theta-\theta_{on})\\ f_{\mathrm{fall}}(\theta)=\frac{T^{*}}{2}+\frac{T^{*}}{2}\cos\frac{\pi}{\theta_{ov}}(\theta-\theta_{off})\end{cases} \quad (3)$$

where $\theta_{on},\theta_{off},\theta_{ov},\theta_{p}$ represent the switch-on, switch-off, overlap, and rotor pitch angles. For an 8/6 SRM, the rotor pitch angle is 30° and the conduction angle θ_{cnd} is 15°. The overlap angle is determined according to equation (4):

$$\theta_{ov}\le\frac{\theta_{p}}{2}-\theta_{off} \quad (4)$$

However, the Conventional TSF method exhibits several limitations that hinder its performance across varying operating conditions. Firstly, it fails to adequately mitigate torque ripple during the commutation overlap region due to its fixed and non-adaptive functional shape[23]. In addition, the performance of TSF is highly sensitive to the choice of switch-on, switch-off, and overlap angles. Therefore, to overcome these challenges, a Gray Wolf Optimization algorithm [24] has been employed in this work to optimize switching angles and overlap angles of the TSF approach. This enhances torque smoothness, reduces ripple, and ensures reliable performance during the entire range of operating conditions.

C. Improved DITC based on optimal TSF using Gray wolf algorithm

To address the issues of torque ripple and reduction output torque in the commutation region in conventional DITC, an optimal TSF based on the DIT C strategy has been proposed in this work. Firstly, this method incorporates the TSF with direct instantaneous torque control (DITC) to achieve effective torque tracking by ensuring that the instantaneous total torque remains constant through distributed phase torque control, which leads to minimized torque ripple. Figure 3 depicts the control diagram of the optimal TSF+DITC strategy of SRM.

Where the total reference torque T_{e}^{*} is attained by the PI controller based on the error between reference speed and actual speed. Subsequently, the phase reference torques $(T_{\mathrm{a}}^{*},T_{\mathrm{b}}^{*},T_{\mathrm{c}}^{*},T_{\mathrm{d}}^{*})$ are generated by TSF to track the total reference torque effectively. Then, the torque error between the estimated torque values $(T_{\mathrm{a}},T_{\mathrm{b}},T_{\mathrm{c}},T_{\mathrm{d}})$ and the reference torque values $(T_{\mathrm{a}}^{*},T_{\mathrm{b}}^{*},T_{\mathrm{c}}^{*},T_{\mathrm{d}}^{*})$ are fed into the hysteresis controller. Finally, the switching state of each phase winding $(S_{\mathrm{a}},S_{\mathrm{b}},S_{\mathrm{c}},S_{\mathrm{d}})$ is produced to asymmetrical bridge power converter according to the soft switching mode of the hysteresis control unit.

Then, Optimizing TSF parameters plays a crucial role in shaping the phase torque profiles and allows for more effective torque-sharing among phases during a wide range of operating conditions, further reducing torque ripple and enhancing the performance of SRMs. In this paper, a Gray wolf algorithm has been employed to optimize the switch-on, switch-off and overlap angle based on a multi-objective function as follows:

$$F_{obj}=min\left(w_{r}\frac{T_{r}}{T_{rb}}+w_{\eta}\frac{\eta_{b}}{\eta}\right);\ w_{r}+w_{\eta}=1 \quad (5)$$

Where, F_{obj}, is the objective function value. w_r and w_η represent the weighting coefficients for torque ripple and efficiency, respectively. T_{rb} and η_b are the base values of T_r and η, respectively. Where the key performance metrics, including average torque ($\mathrm{T_{av}}$), torque ripple ($\mathrm{T_r}$), and efficiency (η), to assess machine performance, can be computed over one electric cycle (τ) as follows [10]:

$$\mathrm{T_{av}}=\frac{1}{\tau}\int_{0}^{\tau}\mathrm{T_e(t)dt} \quad (6)$$

$$\mathrm{T_r}=\frac{\mathrm{T_{max}}-\mathrm{T_{min}}}{\mathrm{T_{av}}} \quad (7)$$

$$\eta=\frac{\omega_{\mathrm{m}}\mathrm{T_{av}}}{\mathrm{V_{dc}I_{av}}} \quad (8)$$

The optimization algorithm performs the offline training of the switch-on (θ_{on}), switch-off (θ_{off}) and overlap angle (θ_{ov}) as a function of reference speed and reference torque (ω*, $\mathrm{T_{ref}}$), as demonstrated in the flowchart of the GWO algorithm in Fig. 4 [25]. In addition, two constraints are subjected to optimized the control parameters; firstly, the minimum conduction angle (θ_{cnd}) for three-phase 12/8 SRM should be at least 15. Moreover, the overlap angle (θ_{ov}) should be tuned according to equation (4).

The GWO algorithm is initially linked to the SRM drive system through the objective function in (5) to train the TSF parameters at different operating points(ω*,$\mathrm{T_{ref}}$). The operating speed (ω*) is between 200-3000 rpm, and the range for the reference torque ($\mathrm{T_{ref}}$) is between 3-30 Nm. The optimization algorithm is carried out at each speed and torque step of 200 rpm and 3Nm. The GWO algorithm selects grey wolves (GW) to be 50, and the maximum number of iterations(S) is 80. Then, the optimal value of control parameters (θ_{on}, θ_{off} and θ_{ov}) are stored in a look-up table (LUT) to be employed later for implementing the suggested approach, as depicted in Figure 3.

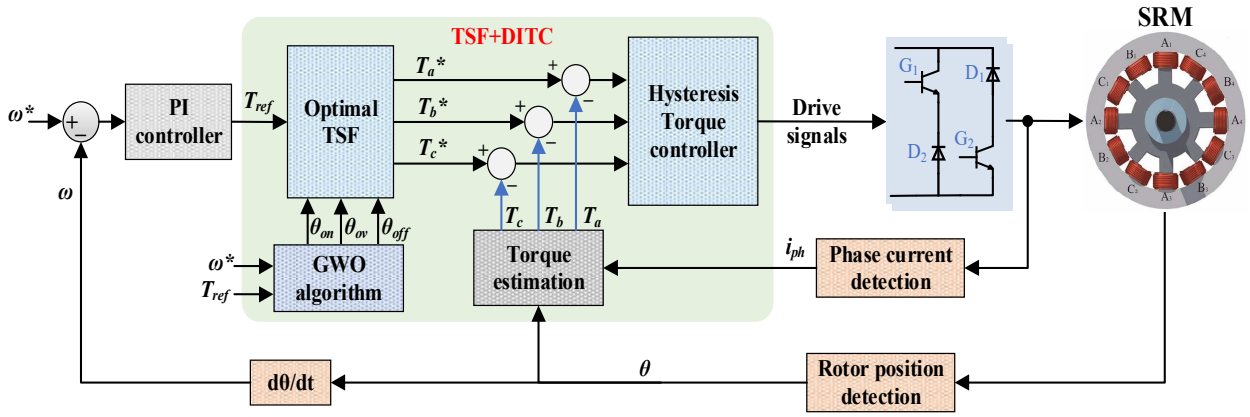

Fig. 3. Proposed optimal TSF+DITC strategy using GWO algorithm for SRM

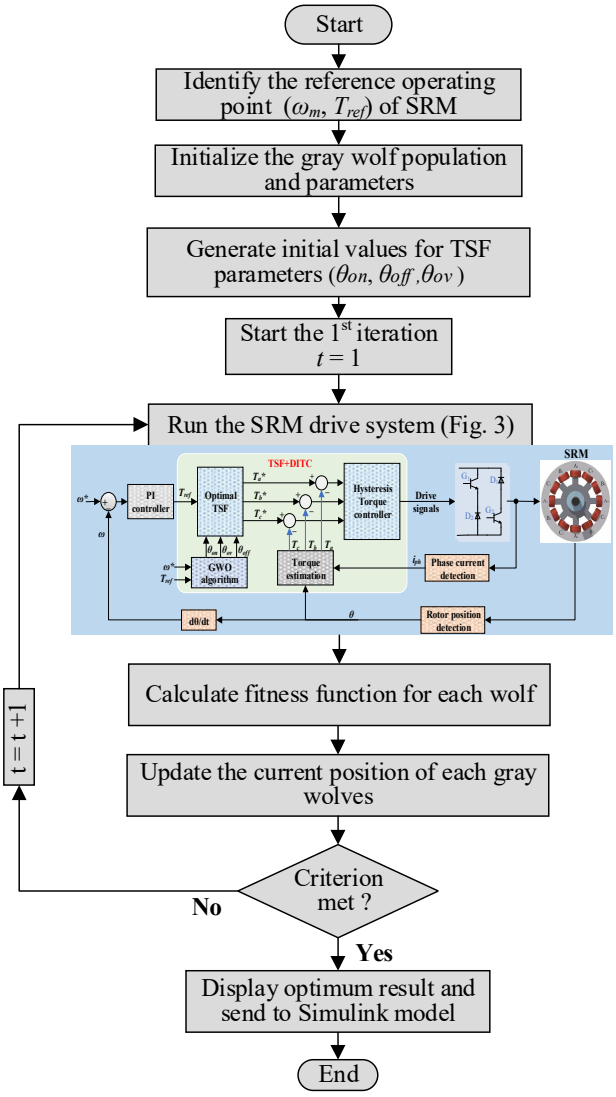

Fig. 4. Flowchart of GWO algorithm

III. Simulation Results

To validate the effectiveness of the proposed optimal TSF+DITC approach, different simulation results have been performed in MATLAB and compared with the optimized DITC method based on ANN [15] by employing an 8/6 SRM. The parameters of the four-phase SRM are listed in Table 1. The machine model is implemented by employing the look-up tables that contain the torque, current and flux characteristics.

TABLE I. The main parameters of SRM

Parameter	Value	Parameter	Value
Output power (kw)	4	Phase Resistance (Ω)	0.642
Terminal voltage (V_{dc})	600	Turn per pole	88
Rated speed (rpm)	1500	Stator outer/ bore diameters	179.5/96.7
Rated Torque (Nm)	26	Height of stator /rotor pole	29.3/18.1
Number of phases	4	Stack/ Air-gap lengths	151/0.4
Stator/Rotor poles	8/6	Stator/ rotor pole arcs	20.45°/21.5°

The performance of the machine has been analyzed and compared across various operating points, specifically selected to represent low (500 rpm), medium (1500 rpm), and high (2300 rpm) speeds, each associated with constant reference torque values of 26 Nm, 22 Nm, and 14 Nm, respectively. The corresponding results are depicted in Figures 5–7. It is important to highlight that the thresholds of the inner and outer hysteresis bands for the torque controller were set to 0.2 Nm and 0.4 Nm, respectively, while the control circuit is set with a sampling time of 10 µs.

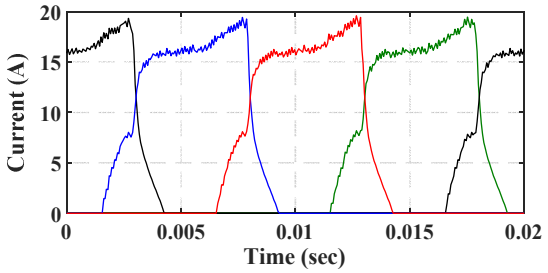

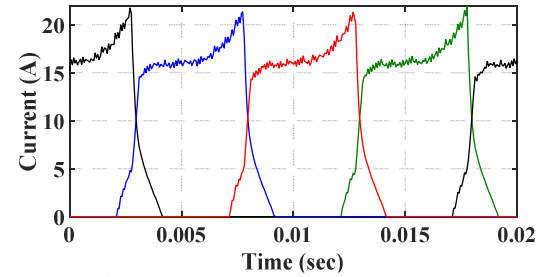

(a) Current waveform of optimal TSF+ DITC

(b) Current waveform of optimized DITC

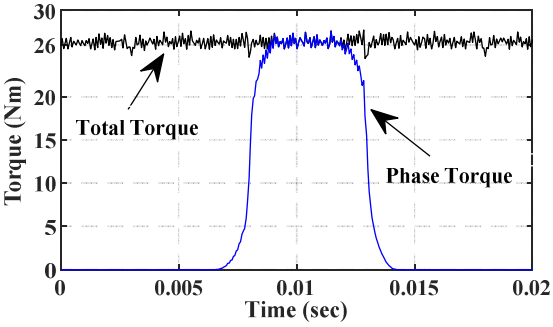

(c) Total torque of optimal TSF+ DITC

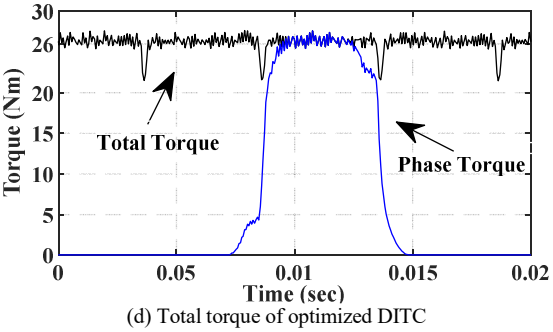

(d) Total torque of optimized DITC

Fig. 5. Simulation results at a speed of 500rpm and 26 Nm reference torque

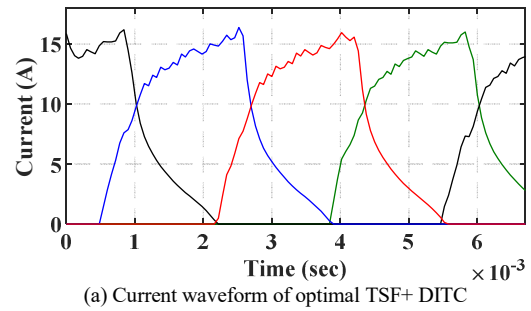

(a) Current waveform of optimal TSF+ DITC

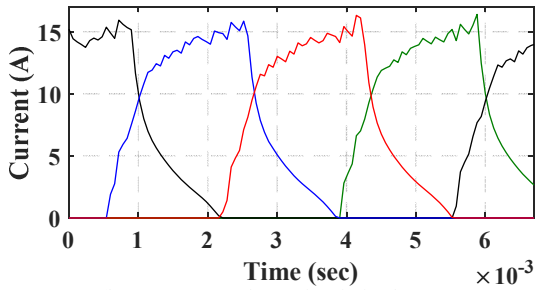

(b) Current waveform of optimized DITC

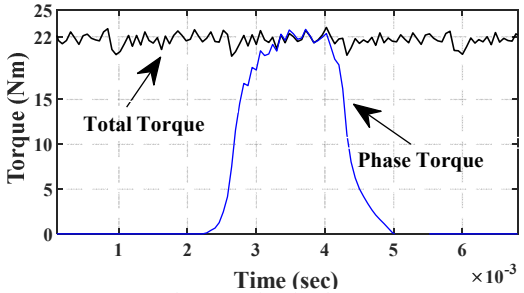

(c) Total torque of optimal TSF+ DITC

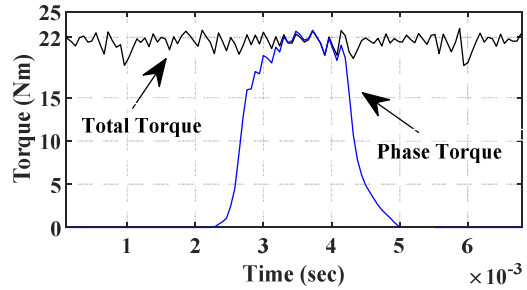

(d) Total torque of optimized DITC

Fig. 6. Simulation results at a speed of 1500rpm and 22Nm reference torque

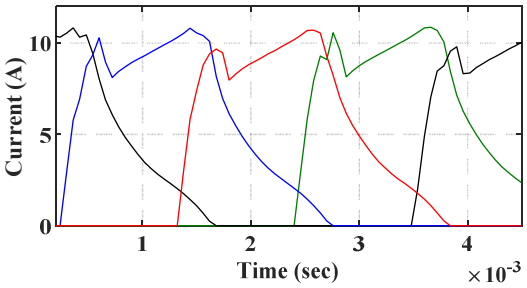

(a) Current waveform of optimal TSF+ DITC

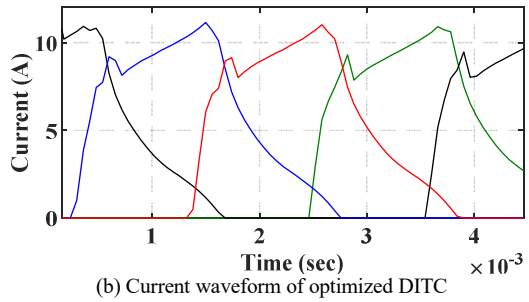

(b) Current waveform of optimized DITC

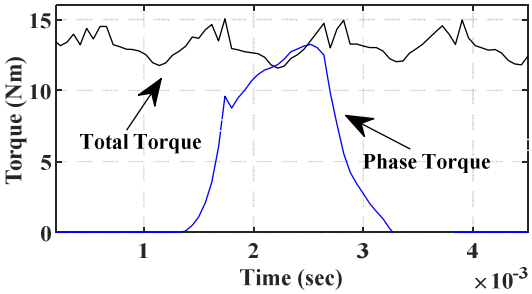

(c) Total torque of optimal TSF+ DITC

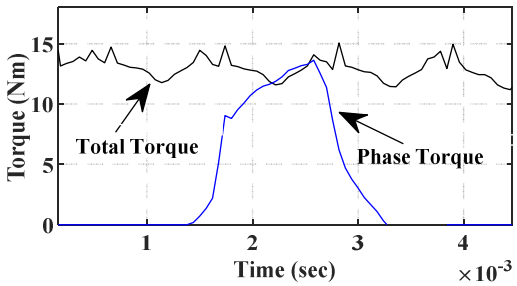

(d) Total torque of optimized DITC

Fig. 7. Simulation results at a speed of 2300 rpm and 14 Nm reference torque

Table II demonstrates a comparative analysis between the proposed strategy and the optimized DITC approach at various operating points.

TABLE II. Comparative results under steady state

Control scheme	ω (rpm)	T_{ref} (Nm)	T_r (%)	T_{av} (Nm)	η (%)
Proposed TSF+DITC	200 rpm	26	16.5	26.42	76.5
Optimized DITC			23.9	26.4	76.4
Proposed TSF+DITC	500 rpm	26	16.2	26.3	84.95
Optimized DITC			22.7	26.26	84.7
Proposed TSF+DITC	1500 rpm	22	17.6	21.67	91.53
Optimized DITC			20.9	21.7	91.54
Proposed TSF+DITC	2300 rpm	14	28.5	13.07	91.08
Optimized DITC			30	13.16	91.21

As illustrated in Figures 5–7 and Table II, the proposed optimal TSF+DITC method demonstrates a significant reduction in torque ripple, improved efficiency, and an enhanced torque profile compared to the optimized DITC approach. The proposed method reduces ripple significantly (by about 7.4%, 6.5%, 3.3%, 1.5%) at speeds (200 rpm, 500 rpm,1500 rpm,2300 rpm), respectively, when compared to the optimized DITC approach. While both suggested approaches maintain very similar average torque at all ranges of speeds, the differences are tiny (on the order of 0.1 Nm or less). Therefore, torque capability is retained. In addition, the proposed strategy slightly enhances efficiency at low speeds (200 rpm and 500 rpm), with comparable values at medium to high speeds (within 0.2%).

The dynamic performance of the proposed approach is evaluated through two test scenarios. In the first test, the motor is subjected to a constant load torque of 26 Nm while experiencing a step change in the reference speed from 1000 rpm to 2000 rpm, as illustrated in Figure 8. In the second test, the motor operates at a constant speed of 1600 rpm and undergoes a step change in the load torque from 10 Nm to 20 Nm, as shown in Figure 9. As demonstrated in Figs. 8(a, b) and 9(a, b), the optimal TSF provides a good torque profile to achieve an excellent tracking response for both sudden changes in speed and load torque.

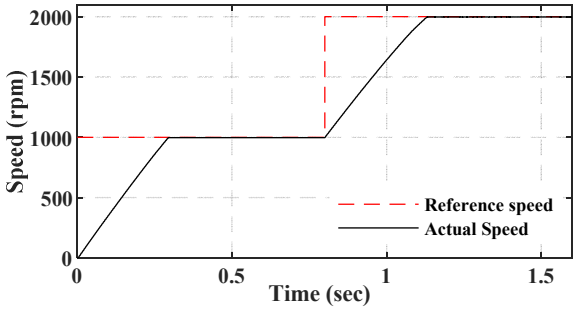

(a) Step change in speed

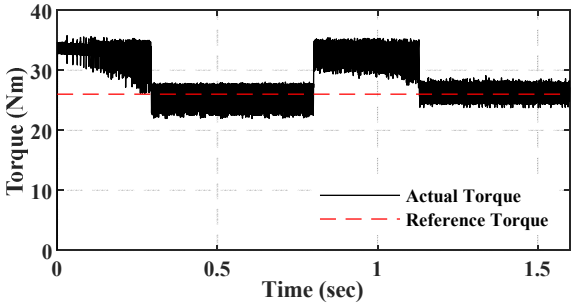

(b) Total torque response

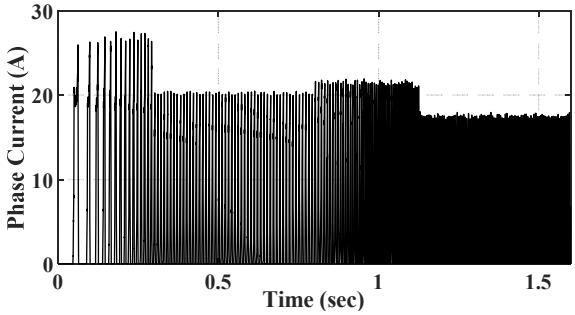

(c) The phase current waveform

Fig. 8. The dynamic response at a step change in speed with a constant load of 26 Nm.

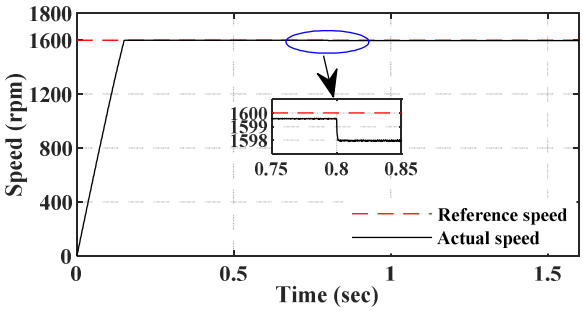

(a) Speed response

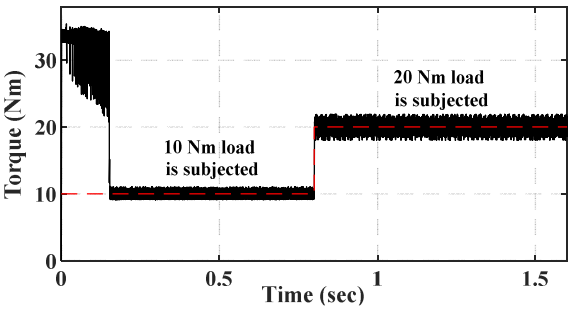

(b) Step change in torque load

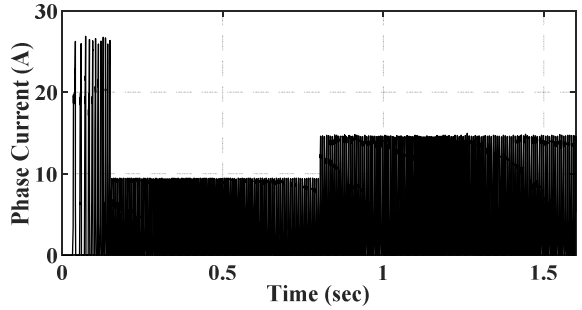

(c) The phase current waveform

Fig. 9. The dynamic response at a step change in torque load with a constant speed of 1600 rpm

IV. Conclusion

This study proposes an enhanced DITC strategy integrated with an optimal TSF approach to address the challenge of torque ripple and reduction in output torque in SRM. A Gray wolf algorithm has been employed to optimize the control parameters of TSF based on the multi-objective function to achieve optimal TSF approach performance. The proposed approach combines the merits of the DITC strategy and the TSF approach to ensure effective phase torque distribution, thereby maintaining a constant instantaneous total torque which leads to minimizing the torque ripple. Finally, the simulation results prove that the suggested approach has reduced the torque ripple more effectively than the traditional control method under step changes in speed and load torque.

References

[1] G. Fang, F. Pinarello Scalcon, D. Xiao, R. Vieira, H. Grundling, and A. Emadi, "Advanced Control of Switched Reluctance Motors (SRMs): A Review on Current Regulation, Torque Control and Vibration Suppression," *IEEE Open Journal of the Industrial Electronics Society*, vol. 2, pp. 280–301, 2021, doi: 10.1109/OJIES.2021.3076807.

[2] A. Seshadri and N. C. Lenin, "Review based on losses, torque ripple, vibration and noise in switched reluctance motor," *IET Electr Power Appl*, vol. 14, no. 8, pp. 1458–1468, Aug. 2020, doi: 10.1049/iet-epa.2019.0251.

[3] M. Abdalmagid, E. Sayed, M. H. Bakr, and A. Emadi, "Geometry and Topology Optimization of Switched Reluctance Machines: A Review," 2022, *Institute of Electrical and Electronics Engineers Inc.* doi: 10.1109/ACCESS.2022.3140440.

[4] K. Diao, X. Sun, G. Bramerdorfer, Y. Cai, G. Lei, and L. Chen, "Design optimization of switched reluctance machines for performance and reliability enhancements: A review," Oct. 01, 2022, *Elsevier Ltd*. doi: 10.1016/j.rser.2022.112785.

[5] A. M. Ajamloo, M. N. Ibrahim, and P. Sergeant, "Design, Modelling and Optimization of a High Power Density Axial Flux SRM with Reduced Torque Ripple for Electric Vehicles," *Machines*, vol. 11, no. 7, Jul. 2023, doi: 10.3390/machines11070759.

[6] A. L. Saleh, F. Al-Amyal, and L. Számel, "Control techniques of switched reluctance motors in electric vehicle applications: A review on torque ripple reduction strategies," 2024, *American Institute of Mathematical Sciences*. doi: 10.3934/electreng.2024005.

[7] C. Gan, J. Wu, Q. Sun, W. Kong, H. Li, and Y. Hu, "A Review on Machine Topologies and Control Techniques for Low-Noise Switched Reluctance Motors in Electric Vehicle Applications," 2018, *Institute of Electrical and Electronics Engineers Inc.* doi: 10.1109/ACCESS.2018.2837111.

[8] A. Abdel-Aziz, M. Elgenedy, and B. Williams, "Review of Switched Reluctance Motor Converters and Torque Ripple Minimization Techniques for Electric Vehicle Applications," Jul. 01, 2024, *Multidisciplinary Digital Publishing Institute (MDPI)*. doi: 10.3390/en17133263.

[9] A. L. Saleh, F. Al-Amyal, and L. Számel, "An enhanced current chopping control strategy for SRM drives using Harris Hawks optimization algorithm," *ISA Trans*, vol. 150, pp. 338–358, Jul. 2024, doi: 10.1016/j.isatra.2024.05.020.

[10] M. Hamouda, A. A. Menaem, H. Rezk, M. N. Ibrahim, and L. Számel, "Comparative evaluation for an improved direct instantaneous torque control strategy of switched reluctance motor drives for electric vehicles," *Mathematics*, vol. 9, no. 4, pp. 1–17, Feb. 2021, doi: 10.3390/math9040302.

[11] F. Al-Amyal, M. Hamouda, and L. Számel, "Performance improvement based on adaptive commutation strategy for switched reluctance motors using direct torque control," *Alexandria Engineering Journal*, vol. 61, no. 11, pp. 9219–9233, Nov. 2022, doi: 10.1016/j.aej.2022.02.039.

[12] L. Al Quraan, A. L. Saleh, and L. Szamel, "Indirect Instantaneous Torque Control for Switched Reluctance Motor Based on Improved Torque Sharing Function," *IEEE Access*, vol. 12, pp. 11810–11821, 2024, doi: 10.1109/ACCESS.2024.3355389.

[13] Y. Hu, C. Gu, Z. Zhang, Z. Kang, and Y. Li, "Torque Ripple Minimization of Six-Phase Switched Reluctance Motor Based on Enhanced Direct Instantaneous Torque Control," *IEEE Transactions on Transportation Electrification*, vol. 10, no. 2, pp. 4371–4382, 2024, doi: 10.1109/TTE.2023.3308974.

[14] Q. Sun, J. Wu, and C. Gan, "Optimized Direct Instantaneous Torque Control for SRMs with Efficiency Improvement," *IEEE Transactions on Industrial Electronics*, vol. 68, no. 3, pp. 2072–2082, Mar. 2021, doi: 10.1109/TIE.2020.2975481.

[15] C. Huang, R. Xiao, C. Gong, and Y. Xiao, "A Novel Direct Instantaneous Torque Control Strategy of Permanent Magnet-Assisted Switched Reluctance Motor with Zero Voltage Modulation," *Progress In Electromagnetics Research C*, vol. 148, pp. 71–82, 2024, doi: 10.2528/PIERC24062801.

[16] A. L. Saleh and L. Számel, "Improved Direct Instantaneous Torque Control Strategy of Switched Reluctance Motor based on Artificial Neural Network," in *2024 6th Global Power, Energy and Communication Conference (GPECOM)*, 2024, pp. 166–172. doi: 10.1109/GPECOM61896.2024.10582580.

[17] S. Wang, Z. Hu, and X. Cui, "Research on Novel Direct Instantaneous Torque Control Strategy for Switched Reluctance Motor," *IEEE Access*, vol. 8, pp. 66910–66916, 2020, doi: 10.1109/ACCESS.2020.2986393.

[18] P. Ren, J. Zhu, Z. Jing, Z. Guo, and A. Xu, "Improved DITC strategy of switched reluctance motor based on adaptive turn-on angle TSF," *Energy Reports*, vol. 8, pp. 1336–1343, Nov. 2022, doi: 10.1016/j.egyr.2022.08.076.

[19] H. Wang, J. Wu, C. Xie, and Z. Guo, "Vehicle-Mounted SRM DITC Strategy Based on Optimal Switching Angle TSF," *World Electric Vehicle Journal*, vol. 16, no. 1, Jan. 2025, doi: 10.3390/wevj16010026.

[20] S. Y. Wang, F. Y. Liu, and J. H. Chou, "Adaptive TSK fuzzy sliding mode control design for switched reluctance motor DTC drive systems with torque sensorless strategy," *Applied Soft Computing Journal*, vol. 66, pp. 278–291, May 2018, doi: 10.1016/j.asoc.2018.02.023.

[21] X. Song, J. Zhu, P. Ren, and X. Lv, "An improved fuzzy control for switched reluctance motor based on torque sharing function," in *Proceedings - 2021 6th International Conference on Automation, Control and Robotics Engineering, CACRE 2021*, Institute of Electrical and Electronics Engineers Inc., 2021, pp. 119–123. doi: 10.1109/CACRE52464.2021.9501376.

[22] W. Cao, C. Huang, Y. Wu, and W. Xie, "Adaptive Torque Sharing Function Control Strategy of Switched Reluctance Motor Based On Neural Network," in *Proceedings of 2022 IEEE 5th International Electrical and Energy Conference, CIEEC 2022*, Institute of Electrical and Electronics Engineers Inc., 2022, pp. 423–428. doi: 10.1109/CIEEC54735.2022.9846184.

[23] X. Sun, Y. Xiong, M. Yao, X. Tang, and X. Tian, "A unified control method combined with improved TSF and LADRC for SRMs Using modified grey wolf optimization algorithm," *ISA Trans*, vol. 131, pp. 662–671, Dec. 2022, doi: 10.1016/j.isatra.2022.05.013.

[24] M. A. Kamoona, J. Manuel Mauricio, A. L. Saleh, and L. Számel, "Advanced MPPT Strategy for PV Solar Energy Systems Using ANN-GWO," in *Proceedings - 2024 IEEE 6th Global Power, Energy and Communication Conference, GPECOM 2024*, Institute of Electrical and Electronics Engineers Inc., 2024, pp. 439–444. doi: 10.1109/GPECOM61896.2024.10582686.

[25] Hassan S. Ahmed, Ahmed J. Abid, Adel A. Obed, Ameer L. Saleh, and Reheel J. Hassoon, "Maximizing Energy Output of Photovoltaic Systems: Hybrid PSO-GWO-CS Optimization Approach," *Journal of Techniques*, vol. 5, no. 3, pp. 174–184, Sep. 2023, doi: 10.51173/jt.v5i3.1312.